Electrochemical Behavior and Corrosion Inhibition of Al and Al-Si Alloy in Inorganic Acidic Solutions

R. M. Abou Shahba[1], A. S. Ibrahim[1], W. A. Hussein[1] N. K. Shehata[1], and W. A. Ghanem[2]

[1]Chemistry Department, Faculty of Science (Girls), Al-Azhar University, Nasr City, Cairo, Egypt
[2]Central Metallurgical Research and Development Institute (CMRDI).Tepen, Cairo, Egypt
wallaahmed@yahoo.com

Abstract: The electrochemical behavior of pure Al and Al-3%Si alloy was studied in some inorganic acid solutions; H_2SO_4, H_3PO_4, HNO_3 and HCL, in absence and presence of some surfactants using open-circuit and potentiodynamic techniques. The evolution of the electrodes surface was examined by scanning electron microscopy (SEM). Al-3%Si electrode becomes passive with lower corrosion current density than pure Al electrode due to the higher Si, Fe and Ti contents. The addition of surfactants leads in all cases to the inhibition of the corrosion process. The results obtained indicated that the inhibition efficiency increased with increasing inhibitor concentration. Also, it was found that, sulfonic acid is more effective to inhibit the corrosion than sodium dodecyl sulphate. The inhibition process was attributed to the formation of adsorbed film on the metal surface that protects the metal against corrosive agents. The sigmoidal shape of the adsorption isotherm confirm the applicability of Langmuir and Temkin equations to describe the adsorption process of the two surfactant tested in 0.1M of the used acid solution on the two aluminum electrodes.

[R. M. Abou Shahba, A. S. Ibrahim, W. A. Hussein, N. K. Shehata, and W. A. Ghanem. **Electrochemical Behavior and Corrosion Inhibition of Al and Al-Si Alloy in Inorganic Acidic Solutions**. *Researcher*. 2011;3(12):92-105]. (ISSN: 1553-9865). http://www.sciencepub.net. 16

Keywords: aluminum; aluminum alloys; Corrosion; inhibition; polarization; Surfactant

1. Introduction

Aluminum and its alloys have remarkable economic and attractive materials for engineering applications owing to its low cost, high weight, high thermal and electrical conductivity. The interest of the materials arises from their importance in recent civilization[1, 2]. The resistance of aluminum against corrosion in aqueous media can be attributed to the rapidly formed surface oxide film. Therefore, aluminum has been known to exhibit widely different electrochemical properties in different aqueous electrolytes[3]. Many studies have been devoted to the inhibition of aluminum corrosion in acidic media by organic compounds, but surfactants have been relatively little studied.

In this work, the authors present a study of the electrochemical behavior of Al and Al-3%Si alloy in some inorganic acid and evaluate the inhibiting effect of some surfactants.

2. Experimental:

Materials:

Two samples of aluminum electrodes of special grades have been tested. Typical values of their chemical compositions are given in Table (1).

Table (1): The chemical composition of aluminum electrodes (by wt. %)

Samples	Al	Si	Fe	Cu	Mn	Mg	Zn	Cr	Ni	Ti	Pb	V
Electrode (I)	99.8	0.040	0.038	0.015	0.0051	0.0074	0.0114	0.001	0.003	0.01	0.005	0.0057
Electrode (II)	95.8	**3.58**	**0.335**	0.014	0.013	0.005	0.025	0.012	0.008	**0.106**	0.010	0.008

Cylindrical electrodes with a working surface area of 1cm^2 were used. Electrodes were enclosed in a glass tube fixing with araldite adhesive. The electrical contact was made through a thick copper wire soldered to inner side of electrode. Prior to each experiment, the surface of the working electrode was prepared by polishing with a sequence of emery paper (600, 800, 1000 and 1200), cleaning several times with deionized water and drying with acetone before immersing in test solution.

Adopted Techniques:

I. Open–Circuit Technique:

Open-circuit measurements were measured in different concentrations of acidic solutions H_2SO_4, H_3PO_4, HNO_3 and HCl (1×10^{-3} to 1M). All measurements were carried out in convinantional glass cell at room temperature. The potential was recorded as a function of time till steady state values were observed by using electronic multimeter. The

potentials were recorded with respect to a saturated calomel electrode (SCE).

II. Potentiodynamic Polarization Technique:

Anodic and cathodic potentiodynamic polarization scans were performed with electronic potentioscan (Volta Lab 40 (PGZ301) – Radiometer analytical). A single compartment–cylindrical three electrodes glass cell of 250 ml capacity was used. All potentials were measured with respect to saturated calomel electrode (SCE) and platinum sheet used as auxiliary electrode. All measurements were performed in freshly prepared aerated solutions at room temperature (25 ± 2°C). The anodic E/I curve for all solutions were swept from -2000 to 1500mV with scan rate of 2mV/s.

The percentage inhibition efficiency (%IE) and degree of surface coverage (θ) of the investigated surfactant compounds were calculated from the following equations:

$$\%IE = [1- (i_{corr\ (inh)} / i_{corr\ (free)})] \times 100 \quad (1)$$

$$\theta = [1- (i_{corr\ (inh)} / i_{corr\ (free)})] \quad (2)$$

Where $i_{corr\ (free)}$ and $i_{corr(inh)}$ are the corrosion current densities in absence and presence of inhibitors.

3. Result and Discussion:

I. Open–Circuit measurements:

Fig.(1-8) represent the variation of the steady state potential of two aluminum electrodes (I and II) with time in different concentrations of H_2SO_4, H_3PO_4, HNO_3 and HCl (1×10^{-3} to 1M) solutions. Accordingly, the behavior is differing depending upon the mode of variation of the steady state potentials with time and concentration of the test solutions.

In H_2SO_4 acid solution, The open circuit potentials of electrode (I) have always a general tendency to drift to more negative values at which it tend to be stabilized after 15-25 minutes, denoting the destruction of the pre-immersion oxide film formed on the surface of the electrode. However, the open-circuit potential of aluminum electrode (II) shifted with time towards more positive values denoting passivation and according to Evans[4] that the oxide film is self-healing.

In H_3PO_4 acid solution and for two electrode type, that the open-circuit potential have a tendency to decrease sharply towards more negative potential until minimum values took place after about 5 minutes, then the potential was slowly increased until a plateau value is reached in a period of time from 5 to 30 minutes.

In HNO_3 acid solution, the open-circuit potential of two electrodes shifts rapidly towards more positive values in a period of about 3 minutes, after which a steady state potential is reached.

For electrode type (I) in concentrated solutions of HCl (0.1-1.0M) the open circuit potential is shifted from positive to more negative values than the initial potential denoting the destruction of the pre-immersion oxide film present on the electrode surface, then increased generally until it reached a steady state potential. However, electrode (I) in low concentrations (0.001- 0.01M), the potential shifts with time towards more positive values, and then it tend to be stabilized after 25 minutes. For aluminum electrode (II), the initial open-circuit potential tends to become more negative until the steady state potential is reached.

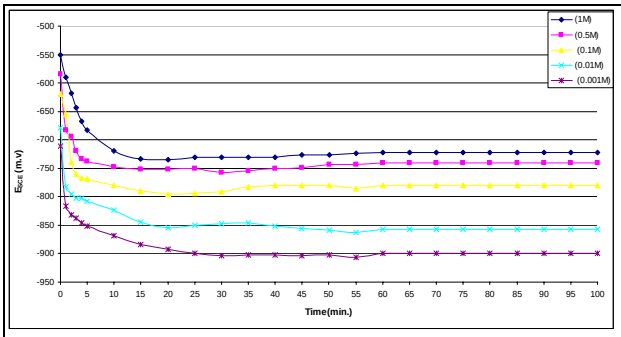

Fig (1) : Potential / Time curve of electrode I in different H_2SO_4 concentrations

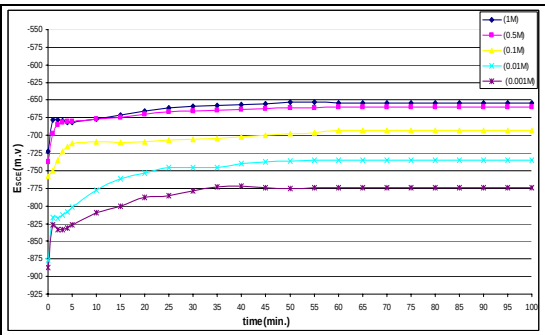

Fig(2) : Potential /Time curve of electrode II in different H_2SO_4 concentrations

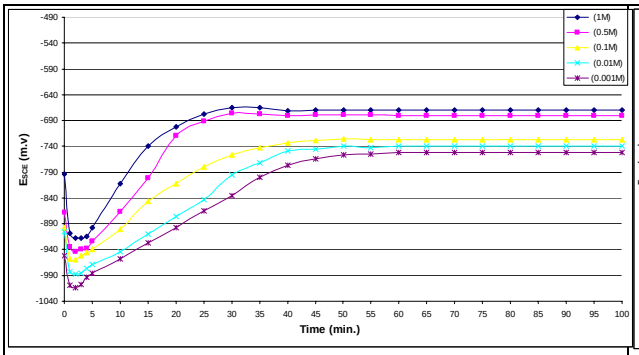

Fig (3) : Potential / Time curve of electrode I in different H_3PO_4 concentrations

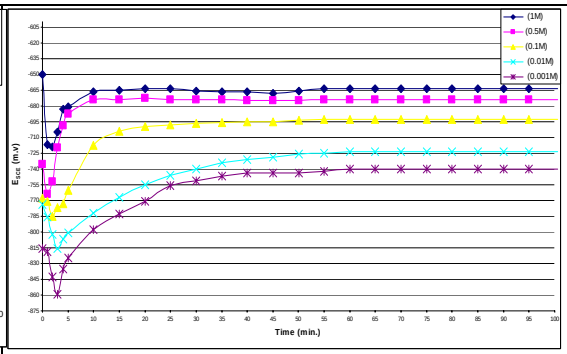

Fig (4) : Potential / Time curve of electrode II in different H_3PO_4 concentrations

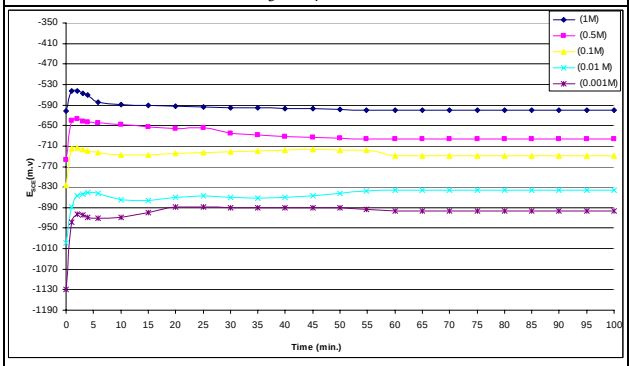

Fig (5) : Potential / Time curve of electrode I in different HNO_3 concentrations

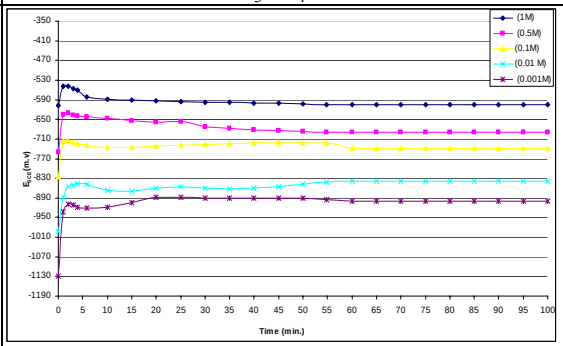

Fig (6) : Potential / Time curve of electrode II in different HNO_3 concentrations

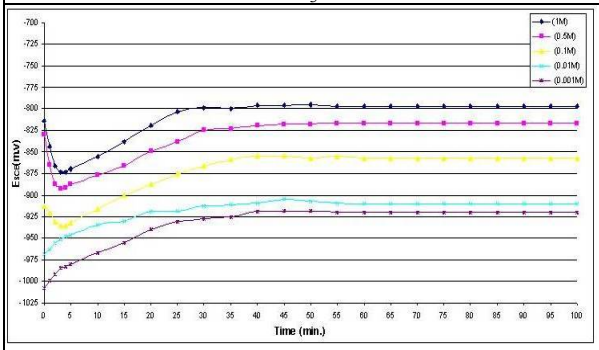

Fig (7) : Potential / Time curve of electrode I in different HCl concentrations

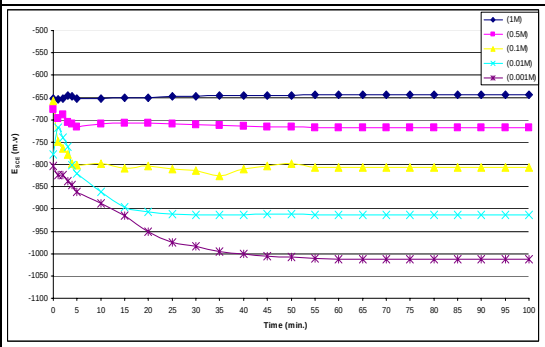

Fig (8) : Potential / Time curve of electrode II in different HCl concentrations

Bracher[5] found that the steady – state potential, $E_{S.S}$, of a number of metal electrodes measured in aerated solutions of a number of anions changes with the anions concentration according to :

$$E_{S.S.} = a - b \log C \qquad (3)$$

Where a and b are constants depending on the type of test solutions.

Depending on the variation of the steady – state potential of metal electrodes with logarithmic molar concentration, Figs.(9-12), (a) can be calculated from the lines making the best fit with experimental results in solution of 1.0M concentration[5]. The values of (a) are: H_2SO_4 (-0.722 and -0.654V), H_3PO_4 (-0.670 and -0.664V), HNO_3 (-0.605 and -0.525V), HCl (-0.797 and -0.644V) for aluminum electrodes (I and II), respectively.

The result obtained from Fig.(9-12) show that, the immersion potential and steady - state potential depend on the nature and composition of the aluminum electrodes. Also, comparing the activity of the two electrodes indicates that, the order runs as:

$$I > II$$

Comparing the corrosion activity of two aluminum electrodes in the used test solutions, it is suggested that the order of runs:

for electrodes (I):

$$HCl > H_2SO_4 > H_3PO_4 > HNO_3$$

While, for the electrode type (II):

$$H_3PO_4 > H_2SO_4 > HCl > HNO_3$$

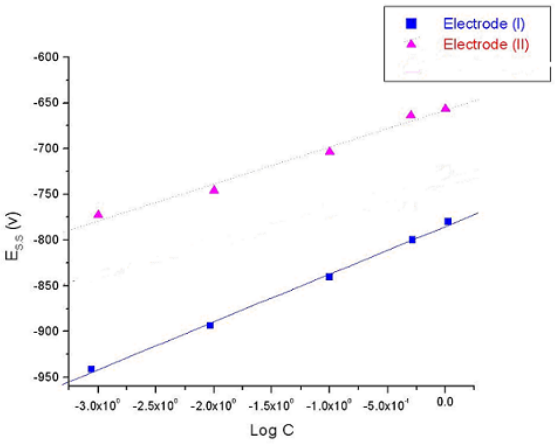

Fig.(9) : $E_{S.S}$/log conc. Curves of electrode (I, II) in different concentrations of H_2SO_4

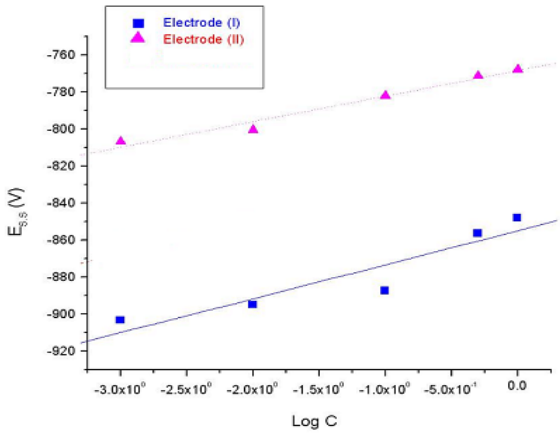

Fig.(10) : $E_{S.S}$/log conc. Curves of electrode (I, II) in different concentrations of H_3PO_4

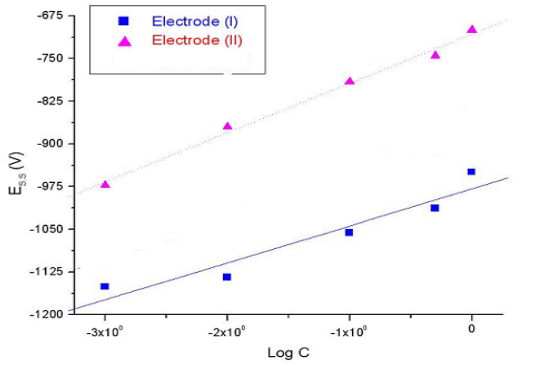

Fig.(11) : $E_{S.S}$/log conc. Curves of electrode (I, II) in different concentrations of HNO_3

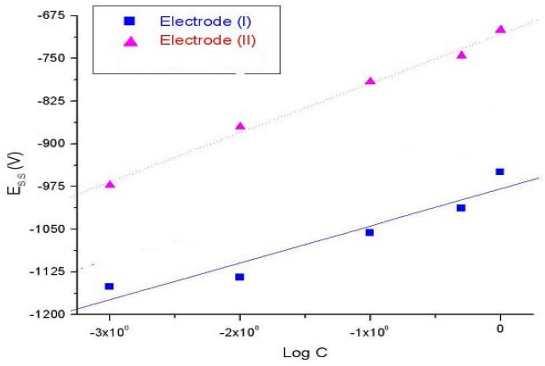

Fig.(12) : $E_{S.S}$/log conc. Curves of electrode (I, II) in different concentrations of HCl

II. Potentiodynamic polarization measurements:

1) In sulphuric acid:

The potentiodynamic anodic and cathodic polarization curves of the two electrodes in H_2SO_4 acid solutions, Fig.(13, 14), reveal that the cathodic current density which corresponds to hydrogen evolution decreases gradually reaching a definite value at the steady state corrosion potential, which depends on the type of the electrode as well as on the acid concentration. The cathodic current density is due to the evolution of hydrogen gas according to the reaction:

$$2H^+_{(oxide)} + 2e^- \rightarrow H_2 \qquad (1)$$

On the other hand, the anodic curves indicated the presence of two distinct regions: the first is characterized by a very small decrease in current density, nearly constant and independent on potential up to a certain critical potential. In the second potential region and in dilute H_2SO_4 solutions (0.001-0.01M) the current, I, would change with the applied potential, E, according to Tafel equation:

$$E = a - b \log I \qquad (3)$$

Where a and b are constants. In more concentrated H_2SO_4 solutions (0.1 – 1.0M) the anodic polarization curves exhibit an apparent Tafel region, and finally a non protective passive region accompanied by a further increase in the applied potential, at nearly constant current density.

The growth of anodic barrier type films on valve metals with implanted radioactive noble gas atoms indicated that both the metal and oxygen ions generally contribute to the charge transport[6-8]. A general mechanism of the charge transport inside the barrier layer is based on the fact that, there are two zones, one adjacent to the oxide – solution interface (oxide dissolution zone) and the other adjacent to the Al-Al_2O_3 interface (oxide formation zone). The

anions which can directly enter the oxide bulk from the oxide – solution interface or from the oxide dissolution zone, under the effect of the field, are OH^- and SO_4^{2-}. Also, from electrochemical reactions e.g. H_2O, OH^-, SO_4^{2-} etc. species, O^{2-} can be produced at the oxide surface. The species OH^-, SO_4^{2-} and O^{2-} under the effect of the high migration together towards the $Al - Al_2O_3$ interface[9].

During migration of the above movable species from the oxide surface towards the $Al–Al_2O_3$ interface the Al^{3+} ions become "stripped" from the surrounding anions in the oxide lattice and solvated by the H_2O and the ion species present in the polarizing solution at the pore bases. This process takes place inside the thin dissolution zone. Then, the solvated Al^{3+} ions move towards the film surface driven by the electric field[9,10]. Due to microcrystalline nature of the oxide the anodic films can grow both by the formation of aluminum oxide at the metal/oxide interface and by precipitation of hydrated aluminum at the solution/oxide interface. The anodizing current is then carried by the flow of SO_4^{2-}, O^{2-}, OH^- and Al^{3+} ions through the film[11].

For the two electrodes, the corrosion rate in 1.0 M H_2SO_4 has higher values than in diluted one. This may be attributed to the composition of the alloys, and formation of complexes with H_2SO_4 solution or soluble sulphate compounds[12].

2) In phosphoric acid:

For electrode (I and in II) in dilute solutions of H_3PO_4 acid, (0.001, 0.01M), the anodic curves indicated three regions, Figs.(15, 16). The first, active dissolution region was observed from -2.0 to -1.25 V_{SCE}. The second region, a current peak signifying the transition from active dissolution to passive state on electrode surface, at -0.85 and from -0.9 to 0.75 V_{SCE}. The third is a trans-passive region from 0.5 to 1.0 V_{SCE}. However, in concentrated solutions, (0.1-1.0 M), no active passive transition was observed and the current seems to be constant at high anodic potential. In addition, it is observed that the hydrogen evolution reaction is activation controlled since the cathodic portions rise to Tafel lines.

In H_3PO_4 acid solutions, Al is oxidized to Al^+ intermediates at metal/oxide interface. The Al^+ intermediates will subsequently be oxidized to Al^{3+} at the oxide/solution interface where also O^{2-} or OH^- is formed. Simultaneously with the formation of O^{2-} ions, hydrogen ions are formed. This results in a local acidification at the oxide/electrolyte interface, resulting in film dissolution. Al^+ and O^{2-} ions must be transported through the oxide layer. This transportation is due to high electric field strength. In acidic solutions, therefore, the positively charged surface sites will electrostatically attract any anions present in solution, and repel cations[13].

Where the composition of electrodes (I and II) have AlFeSi alloy, so, in H_3PO_4 solution, a layer of phosphate is formed on the electrodes surface. There by; the surface pH above the electrodes increases due to the consumption of H^+ causing deposition of insoluble phosphate. No phosphate is observed on the Si-particles because they are electrochemically inactive in acid solutions[14,15]. According to Pourbaix diagram, an electrochemically passive SiO_2 layer easily forms on Si in aqueous solutions. It has been stated that such electrochemically passive layers suppress the rate of cathodic reaction, thus lowering the galvanic effect of Si remarkably[16,17]. The passive film of aluminum electrodes essentially composes from aluminum oxide, aluminum phosphate and silicon oxide with the formation of soluble silicon phosphate which is dissolved in acid solutions and unstable.

3) In nitric acid:

The potentiodynamic polarization curves performed for electrodes (I and II) in HNO_3 solutions, Figs.(17, 18), indicated three regions similar to those observed in H_3PO_4 solutions.

Mechanism for dissolution of aluminum electrodes in nitric acid solutions is assumed to take place according to an autocatalytic mechanism involving the formation of HNO_2 acid. Oxide films formed on aluminum electrodes in HNO_3 solution have the chemical compositions which correspond to the Al oxyhydroxide with the boehmite structure γ-AlOOH[18] or anhydrous γ- Al_2O_3[19]. It is also concluded that the films formed at zero and negative potentials (vs. SCE) consist of an inner layer of γ-Al_2O_3 and outer layer of $Al(OH)_3$. Only at more positive potentials, (0.5 and 1.5 V), the oxide layer is γ-Al_2O_3. An appealing feature of this interpretation is that, one would expect hydroxide at more negative potentials, but oxide at oxidizing positive potentials[20].

The primary process is the displacement of H^+ from solution,

$$H^+ + e^- \longrightarrow H \qquad (2)$$

$$H + HNO_3 \longrightarrow H_2O + NO_2 \qquad (3)$$

The nitrogen dioxide thus produced would be adsorbed on the metal surface where it would be reduced according to,

$$NO_2 + e^- \longrightarrow NO_2^- \qquad (4)$$

This reaction would be followed by,

$$NO_2^- + H^+ \longrightarrow HNO_2 \quad (5)$$

At high acid concentrations the undissociated HNO_2 will react with HNO_3

$$HNO_2 + HNO_3 \longrightarrow 2\,NO_2 + H_2O \quad (6)$$

In this mechanism two molecules are produced while one is consumed.

This increase of NO_2 concentration is responsible for the increase in the rate of dissolution. It can be deduced that the cathodic reduction of nitrate anions on an aluminum oxide surface occurred with a Tafel slope. It is not at this stage known that the reduction product which are possible, including N_2, NH_4^+ and others. It could even be that the reduction of nitrate anions operates synergistically with H^+ reduction [21].

As has been mentioned above for the oxide films studied, there is an anodic dissolution of metal at Al/oxide interface during the polarization, that according to conventional opinion[19, 22, 23], results in the formation of hydrated compounds of aluminum. Thus, it may be suggested that the anodic film grown in nitric acid electrolyte is boehmite like structure, that is, they may represent amorphous boehmite or pseudo-boehmite. Then, another assumption was made also accounting the possible hydration of the anodic film during polarization process in HNO_3 acid solutions. It is supposed that the film might be a composite one, consisting of amorphous alumina and pseudoboehmite[24].

3) In hydrochloric acid:

The E-I curves of electrode (I) as well as electrode (II), Fig.(19, 20), illustrated that the current decreased with increasing applied potential in cathodic portions. This means that the reduction of protons, which transport across the oxide film at microscopic path, obeys the Tafel relationship and the other part of protons absorbed within the oxide film combine with oxygen ions to form hydrogen containing species such as (OH^-) ions and/or water molecules within the oxide film according to the following [25-29]:

$$H^+_{(oxide)} + O^{2-}_{(oxide)} \longrightarrow OH^-_{(oxide)} \quad (7)$$

$$2H^+_{(oxide)} + O^{2-}_{(oxide)} \longrightarrow H_2O_{(oxide)} \quad (8)$$

This idea indicates that the absorption of protons into the oxide film causes a compositional change from the anhydrous oxide (γ-Al_2O_3) to a hydroxide film (hydration) without a cationic valence change[30]:

$$Al_2O_3 + 2H^+ + O^{2-} \longrightarrow 2AlOOH \quad (9)$$

It is conceivable during a sufficiently large cathodic polarization at potentials below the hydrogen evolution potential in acidic solutions; the rate of protons transport across the oxide may be higher than that of the formation of OH^- ions and /or H_2O molecules. This lead to an accumulation of H_2 at the metal/oxide interface, which may cause local breakdown of the film by mechanical stress[31, 32]. Thus, it can be inferred that the current rise and mass-decay is due to enhanced hydrogen evolution at the bottom of micro-pits, formed by local breakdown of the film[31, 32].

An analysis of the polarization curves indicates that at low overpotential, the Tafel relationship is followed, showing that both anodic and cathodic reactions are activation-controlled. At higher overvoltage, a limiting diffusion current appears on the anodic and cathodic polarization curves showing that at higher densities, the transport of ions towards the electrode surface becomes the rate-determining step[33].

The presence of aggressive ions like chloride prevents the formation of the passive film and accelerates the process of anodic dissolution. The pitting corrosion of aluminum is due to the migration of chloride ion through the oxide film or due to the chemisorbed chloride ions onto the oxide surface where there are act like reaction partners, aiding dissolution via the formation of oxide-chloride complexes. Chloride ion is bonded chemically in the interface as an initial step of the formation of different mixed oxo-hydro- and chloro copmlexes according to the following equations[34]:

$$Al\,[O_x(OH)_y\,(H_2O)_z] + Cl^- \longrightarrow Al[O_x(OH)_{y-1}Cl\,(H_2O)_z] + OH \quad (10)$$

$$(AlOOH)_4xH_2O + Cl^- \longrightarrow (AlOOH)_3xAlOClX\,H_2O + OH^- \quad (11)$$

$$AlOOH + Cl^- \longrightarrow AlOCl + OH^- \quad (12)$$

$$Al(OH)_3 + Cl^- \longrightarrow Al(OH)_2Cl + OH^- \quad (13)$$

Finally the $[(AlCl_6)]^{3-}$ complex is produced[34].

By growing pits, the pH is lower than that of the solution and thus, the metal oxidizes with the formation of soluble species. The predominant anodic process in presence of Cl^- ion in pitting conditions is the formation of soluble aluminum chloride, possibly $AlCl_4^-$ or $Al_2O_8^{2-}$, instead of aluminum oxide[34]. Also, high concentrations of chloride, high anodic potentials and the absence of convection induced by simultaneous hydrogen evolution are needed in order to obtain continuous aluminum chloride film formation on the metal[35].

The electrochemical behavior of two electrodes in all acids used showed that, the corrosion potential, $E_{corr.}$, the corrosion current density, $I_{corr.}$, and the corrosion rates, C.R., increased as the concentration of the used acid is increased. It is also observed that corrosion rate of electrode type I is higher than electrode type II.

The presence of Si atoms, which are solid – solutionized in the aluminum, making a protective film on the aluminum alloy surface more stable because of the formation of SiO_2 which is insoluble in all acid solution where Al_2O_3 dissolve[36]. Electrode II becomes passive with lower corrosion current density than electrode I, is due to the higher Si, Fe and Ti contents in grades not only enhances passivity but also retards corrosion in active state. By comparing the corrosion current values for two aluminum electrodes, the order of activity is:

Electrode I > Electrode II

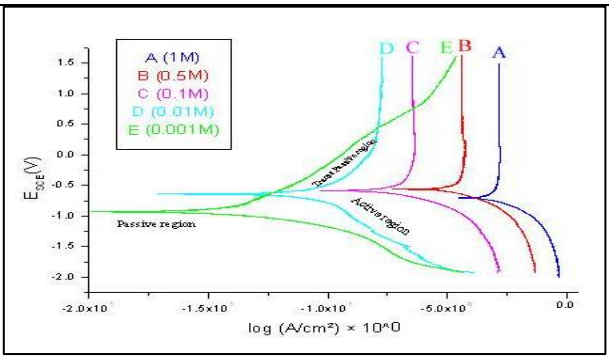

Fig (13) : Anodic and cathodic polarization curves of electrode (I) in H_2SO_4 solutions.

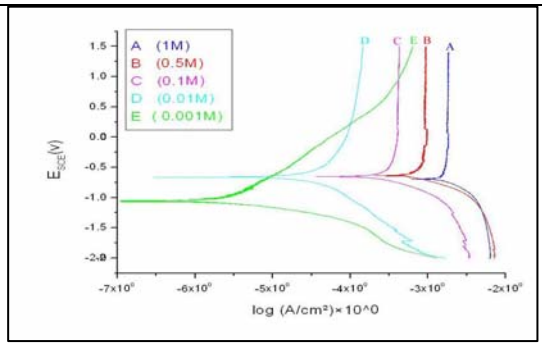

Fig (14) : Anodic and cathodic polarization curves of electrode (II) in H_2SO_4 solutions.

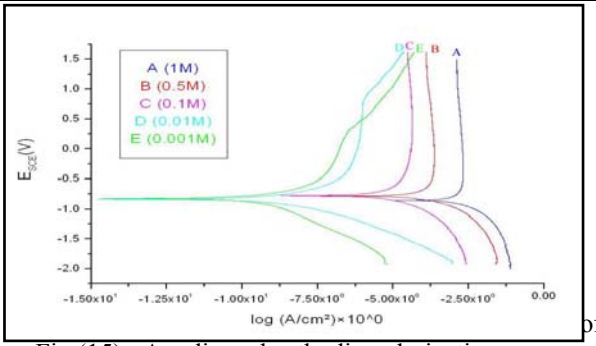

Fig (15) : Anodic and cathodic polarization curves of electrode (I) in H_3PO_4 solutions.

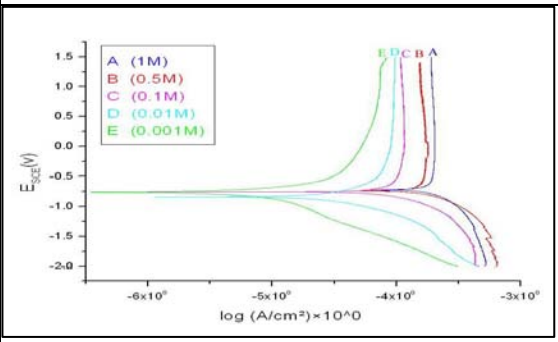

Fig (16) : Anodic and cathodic polarization curves of electrode (II) in H_3PO_4 solutions.

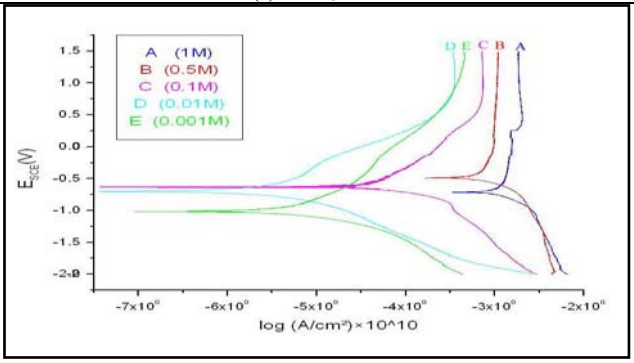

Fig (17) : Anodic and cathodic polarization curves of electrode (I) in HNO_3 solutions.

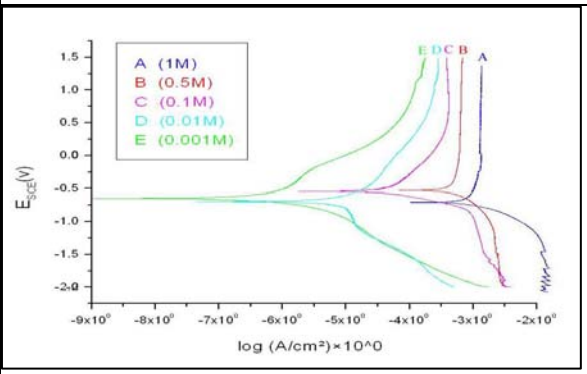

Fig (18) : Anodic and cathodic polarization curves of electrode (II) in HNO_3 solutions.

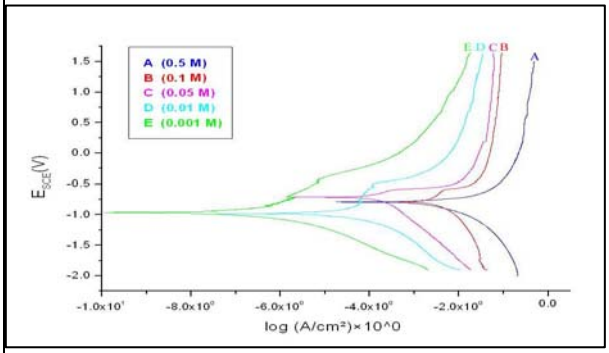

Fig (19) : Anodic and cathodic polarization curves of electrode (I) in HCl solutions.

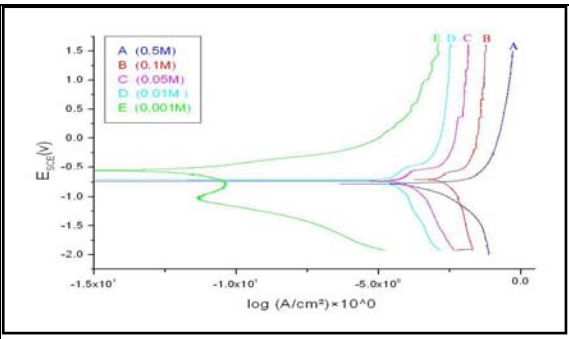

Fig (20) : Anodic and cathodic polarization curves of electrode (II) in HNO_3 solutions.

The role of some organic compounds, such as sulfonic acid and sodium dodecyl sulphate as surfactants solution in the retardation of corrosion of aluminum electrodes in 0.1M H_2SO_4, H_3PO_4, HNO_3 and HCl media were studied. From the electrochemical parameters data, Tables(2, 3), it is clear that, the addition of surfactants enhances both the anodic and cathodic overpotentials (but mainly the cathodic) and increases the polarization resistance (R_P). The open-circuit corrosion potential, $E_{corr.}$, are drifted to more positive values. It is also found that as the concentration of surfactant increased the value of corrosion current, $I_{corr.}$ and corrosion rate values decreased and tend to become more negative. However, the values of corrosion potential, $E_{corr.}$, anodic Tafel slope, cathodic Tafel slope, B_c, inhibition efficiency, polarization resistance and surface coverage values (θ) increased and become more positive as the concentration of the surfactant increased. This indicates that the presence of these compounds retards the dissolution of aluminum in various acidic solutions used by acting predominately as anodic inhibitors; also the suppression of the cathodic process can be due to the coverage of the surface with monolayer of the adsorbed inhibitors molecules.

On the other hand, the presence of Si as an alloying element increases the corrosion resistance of aluminum electrodes II. This was assigned to the incorporation of Si atoms in the natural Al_2O_3 film present on the alloy surface[37]. This incorporation repairs the film defects and precludes significant dissolution of the oxide film by ions[38].

Comparing the inhibition efficiency values for the two electrodes at the same concentration of, (1%), sulfonic acid and sodium dodecyl sulfate it is concluded that the inhibition efficiency decreases in the order:

- sulfonic acid:

For H_2SO_4 acid: Electrode II > Electrode I
For H_3PO_4, HNO_3 and HCl acid:
Electrode I > Electrode II

- Sodium dodecyl sulfate:

For H_2SO_4 and H_3PO_4 acid:
Electrode II > Electrode I
For HNO_3 and HCl acid:
Electrode I > Electrode II

Sulfonic acid molecules probably favor flat orientation on the metal surface to be adsorbed, while sodium dodecyl sulfate molecules probably favor vertical orientation due to steric effect. Thus sulfonic acid is better adsorbed and also has higher inhibition efficiency than sodium dodecyl sulphate[39,40].

III- Adsorption Isotherms:

Langmuir and Temkin adsorption isotherm were found to fit well with the most of the experimental data. According to Langmuir relationship[41]:

$$\text{Log } \theta / (1-\theta) = \text{Log A} + \text{Log C} - Q/ 2.303RT \quad (4)$$

Where θ is the surface covered by the inhibitors and hence (1-θ) is the uncovered surface. A is the adsorption equilibrium constant, C, the bulk concentration of the inhibitors (mole/L) and Q is the heat of adsorption (Kcal/mol).e

The plot of Log θ / (1-θ) vs. Log C for the used inhibitors give straight lines, also the relationship between the adsorption constant and adsorption free energy is given by:

$$K = \exp (-\Delta G^{\circ}_{ads} / RT) \quad (5)$$

Where R is the universal gas constant and T is the absolute temperature.

According to Temkin adsorption isotherm[42] :

$$\ln KC = a\,\theta \quad (6)$$

Where a is a parameter characterizing the interaction between the adsorbed particles and the homogeneity of the surface and is a measure for the steepness of the adsorption isotherm, plot of θ vs. LogC give straight lines.

Table (2): Electrochemical parameters and inhibition efficiency (I.E.%) of electrode (I and II) inH_2SO_4, H_3PO_4, HNO_3 and HCl solutions with (0.25-1%) Sulfonic acid:

Inhibitor used		Media	Conc. (M)	$E_{corr.}$ (V)	$I_{corr.} \times 10^{-3}$ (A/cm^2)	Tafel slopes		θ	R_P K ohm/cm^2	Corrosion rate mm/y	I.E %
						B_a(mv)	B_c(mv)				
Sulfonic Acid	Electrode (I)	H_2SO_4	0.1 thick	-0.6569	5.7975	582.0	-1028.4	----	----	102.7	----
			+0.25 %	-0.7035	0.0584	962.1	-330.4	0.0724	0.6165	6.827	93.3
			+0.5 %	-0.6971	0.01787	1232.3	-316.7	0.7162	0.6793	2.090	97.3
			+1 %	-0.6950	0.01480	1267.9	-300.7	0.7649	1.86	1.731	98.3
		H_3PO_4	0.1 thick	-0.6885	0.1645	2160.6	-530.9	----	----	19.24	----
			+0.25 %	-0.5780	0.01373	659.0	-492.8	0.961	1.98	0.1605	99.1
			+0.5 %	-0.4684	0.01241	672.7	-1341.7	0.991	2.57	0.1451	99.2
			+1 %	-0.1240	0.0104	765.3	-297.3	0.995	6.13	0.1211	99.4
		HNO3H	0.1 thick	-0.6366	0.0465	893.6	-776.4	----	----	5.332	----
			+0.25 %	-0.4992	0.007434	1855.0	-905.3	0.840	0.0025	0.008695	99.8
			+0.5 %	-0.3361	0.002742	1495.5	-784.7	0.941	0.3002	0.003207	99.9
			+1 %	-0.3235	0.000991	569.9	-589.1	0.979	0.7039	0.001159	99.98
		HCl	0.1 thick	-0.9037	0.638	896.3	-757.9	----	----	74.64	----
			+0.25 %	-0.5927	0.0265	162.8	-322.7	0.958	1.19	0.3096	99.5
			+0.5 %	-0.6169	0.0246	171.1	-347.2	0.961	1.62	0.2876	99.6
			+1 %	-0.5815	0.0158	343.3	-584.0	0.975	2.94	0.1846	99.7
	Electrode (II)	H_2SO_4	0.1 thick	-0.6863	6.2964	637.2	-807.5	----	----	94.17	----
			+0.25 %	-0.7143	0.0159	672.6	-281.8	0.179	2.08	15.540	83.5
			+0.5 %	-0.6139	0.01329	434.9	-932.3	0.165	4.03	0.186	99.8
			+1 %	-0.3368	0.0075	227.6	-346.2	0.907	5.19	0.08721	99.9
		H_3PO_4	0.1 thick	-0.8813	1.8488	987.1	-749.0	----	----	2.162	----
			+0.25 %	-0.8435	0.0727	783.0	-324.7	0.747	1.21	0.8506	60.6
			+0.5 %	-0.6181	0.0158	568.7	-349.9	0.901	1.37	0.1842	91.5
			+1 %	-0.5696	0.0099	457.4	-313.6	0.991	1.73	0.1130	94.8
		HNO_3	0.1 thick	-0.5459	0.3719	1072.5	-459.3	----	----	1.34	----
			+0.25 %	-0.5494	0.03630	367.9	-851.6	0.902	0.0035	1.237	7.7
			+0.5 %	-0.5322	0.0106	836.6	-580.9	0.997	6.78	0.4245	68.3
			+1 %	-0.4058	0.0061	239.9	-1487.7	0.981	7.47	0.07132	94.7
		HCl	0.1 thick	-0.7838	0.6978	569.8	-689.8	----	----	8.161	----
			+0.25 %	-1.0189	0.1086	764.8	-294.7	0.844	2.57	1.270	84.4
			+0.5 %	-0.8282	0.0402	252.2	-290.0	0.942	3.61	0.475	94.2
			+1 %	-0.7789	0.0075	440.6	-371.4	0.989	7.48	0.08822	98.9

Table (3): Electrochemical parameters and inhibition efficiency (I.E.%) of electrode (I and II) inH_2SO_4, H_3PO_4, HNO_3 and HCl solutions with (1-3%) sodium dodecyl sulfate:

Inhibitor used		Media	Conc. (M)	$E_{corr.}$ (V)	$I_{corr.}$ x 10^{-3} (A/cm^2)	Tafel slopes		θ	R_P K ohm/cm^2	Corrosion rate mm/y	I.E %
						B_a(mv)	B_c(mv)				
Sodium Dodecyl Sulfate	Electrode (I)	H_2SO_4	0.1 thick	-0.6569	5.7975	582.0	-1028.4	----	----	102.7	----
			+1 %	-0.6788	0.2123	1064.5	-397.0	0.663	0.91129	2.438	97.6
			+2 %	-0.6392	0.0164	519.4	-318.8	0.974	1.67	0.192	99.8
			+3%	-0.5411	0.0122	456.6	-262.2	0.981	2.61	0.143	99.9
		H_3PO_4	0.1 thick	-0.6885	0.1645	2160.6	-530.9	----	----	19.24	----
			+1 %	-0.6694	0.0271	267.3	-475.0	0.985	0.27555	2.317	87.9
			+2 %	-0.6626	0.01679	1941.9	-685.4	0.991	0.91483	1.963	89.8
			+3%	-0.6393	0.01095	771.5	-741.6	0.994	1.59	1.280	93.3
		HNO_3	0.1 thick	-0.6366	0.0465	893.6	-776.4	----	----	5.332	----
			+1 %	-0.5455	0.0101	780.6	-1485.5	0.783	0.0129	0.1182	97.78
			+2 %	-0.2216	0.00612	599.1	-1220.6	0.868	0.0189	0.07164	98.66
			+3%	-0.2108	0.0024	212.3	-794.4	0.948	0.0912	0.02776	99.48
		HCl	0.1 thick	-0.9037	0.638	896.3	-757.9	----	----	74.64	----
			+1 %	-1.1422	0.3862	122.3	-570.6	0.395	0.2992	4.517	93.9
			+2 %	-0.6471	0.1063	476.2	-627.9	0.833	2.44	1.242	98.3
			+3%	-0.6532	0.0147	177.4	-339.8	0.977	3.09	0.1724	99.8
	Electrode (II)	H_2SO_4	0.1 thick	-0.6863	6.2964	637.2	-807.5	----	----	94.17	----
			+1 %	-0.8411	0.017257	1101.1	-893.1	0.786	0.02355	20.18	70.2
			+2 %	-0.0283	0.007685	578.4	-113.9	0.905	0.11188	0.0899	99.86
			+3%	-0.0112	0.00136	576.3	-308.7	0.983	0.46171	0.0159	99.97
		H_3PO_4	0.1 thick	-0.8813	1.8488	987.1	-749.0	----	----	2.162	----
			+1 %	-0.8607	0.3501	2799.8	-705.0	0.836	0.01127	1.869	13.5
			+2 %	-0.2582	0.0177	440.4	-1279.7	0.992	0.01875	0.2015	90.7
			+3%	-0.2117	0.0172	------	-1667.6	0.992	0.68550	0.137	93.7
		HNO_3	0.1 thick	-0.5459	0.3719	1072.5	-459.3	----	----	1.34	----
			+1 %	-1.1343	0.02447	1147.8	-1060.7	0.934	0.8095	0.143	89.3
			+2 %	-0.5822	0.02349	1002.2	-929.8	0.937	0.9783	0.0903	93.3
			+3%	-0.5251	0.01047	787.5	-473.8	0.972	1.31	0.0629	95.3
		HCl	0.1 thick	-0.7838	0.6978	569.8	-689.8	----	----	8.161	----
			+1 %	-1.1370	0.3894	244.4	-604.1	0.442	1.13	4.554	44.2
			+2 %	-1.2723	0.0117	402.5	-341.6	0.973	1.62	0.1367	98.3
			+3%	-0.1506	0.01873	707.4	-723.6	0.983	6.91	0.0219	99.7

As it is clear from data in Table (4, 5), the large values of ΔG°_{ads} and negative sign, obtained from Langmuir and Temkin adsorption isotherms, indicate the adsorption of the two inhibitors on aluminum electrodes surface is spontaneously and accompanied by a highly efficient adsorption. The large negative free energies of adsorption and positive value of heats of adsorption are indication of strong interaction. Also, negative values ΔG°_{ads} indicated that molecular interaction are not predominant in the formation of a protective layer of the inhibitor or its complexes which in turn reduce the corrosion rates[43].

Finally, this led to the conclusion that the positive values of (a) imply the interactions between molecules which causes an increase in the adsorption energy with the increase of θ. As adsorption is Langmuir and Temkin character, the organic molecules are attached as layers and through physical and chemical sorption mechanism[43,44] on the surface and blocking the active sites.

Table(4) Adsorption parametrs obtained from Langmuir and Temkin adsorption isotherms for electrode (I):

Electrode (1)												
Methods	**Langmuir**						**Temkin**					
media	**Sulfonic acid**			**Sodium dodecyl sulfate**			**Sulfonic acid**			**Sodium dodecyl sulfate**		
	K dm^3 mol^{-1}	**q Kcalmol^{-1}**	**$-\Delta G \times 10^{-2}$ KJ mol^{-1}**	**K dm^3 mol^{-1}**	**q Kcal mol^{-1}**	**$-\Delta G \times 10^{-2}$ KJ mol^{-1}**	**K dm^3 mol^{-1}**	**q Kcal mol^{-1}**	**$-\Delta G \times 10^{-2}$ KJ mol^{-1}**	**K dm^3 mol^{-1}**	**q Kcal mol^{-1}**	**$-\Delta G \times 10^{-2}$ KJ mol^{-1}**
H_2SO_4	9.7015	0.6302	5.8227	27.6331	2.6059	8.5050	6.2722	0.8694	4.7051	9.2584	0.6622	5.7029
H_3PO_4	131.1565	2.6280	12.4958	69.8135	−1.2888	10.8799	9.9062	17.7242	5.762	9.6785	−10.7863	5.1867
HNO_3	8.5298	1.9098	5.4929	0.1219	3.0343	−5.3929	9.6063	4.3452	5.7975	1.2459	0.7204	0.5634
HCl	108.4051	2.0271	12.0076	0.5178	3.9003	−1.6866	9.3972	33.2668	5.7411	2.3188	0.2899	2.1552

Table(5) Adsorption parametrs obtained from Langmuir and Temkin adsorption isotherms for electrode (II):

Electrode (I1)												
Methods	**Langmuir**						**Temkin**					
media	**Sulfonic acid**			**Sodium dodecyl sulfate**			**Sulfonic acid**			**Sodium dodecyl sulfate**		
	K dm^3 mol^{-1}	**q Kcalmol^{-1}**	**$-\Delta G \times 10^{-2}$ KJ mol^{-1}**	**K dm^3 mol^{-1}**	**q Kcal mol^{-1}**	**$-\Delta G \times 10^{-2}$ KJ mol^{-1}**	**K dm^3 mol^{-1}**	**q Kcal mol^{-1}**	**$-\Delta G \times 10^{-2}$ KJ mol^{-1}**	**K dm^3 mol^{-1}**	**q Kcal mol^{-1}**	**$-\Delta G \times 10^{-2}$ KJ mol^{-1}**
H_2SO_4	11.5232	2.2738	6.2635	0.4019	2.8512	-2.3359	8.2192	1.7481	5.3979	1.9771	0.774	1.7467
H_3PO_4	96.9393	1.8570	11.7211	6.6032	2.3445	4.8369	8.6447	29.7442	5.5272	7.4534	3.8725	5.1472
HNO_3	4.9192	1.2485	4.0824	0.8091	1.5699	-0.5428	6.2767	1.5601	4.7067	2.8204	1.2793	2.6570
HCl	26.7713	−0.7626	8.4238	80.6102	−0.9605	11.2485	9.9286	297.6190	5.8820	9.7187	−21.3447	5.8273

IV- SEM:

As it is clear from scanning electron microscopy (SEM) for aluminum electrode (II), the microstructure for specimens surface immersed in the used acids, Fig.(21,a,c,e and g), showed heterogeneous surface morphology characterized by groves with some scattered pits. After addition of 3% sodium dodecyl sulphate to plain acid, Fig.(21,b,d,f and h), the attack was reduced and specimen kept their metallic luster with formation of adsorbed layer of the inhibitor on the electrode surface confirming the highest inhibition efficiency.

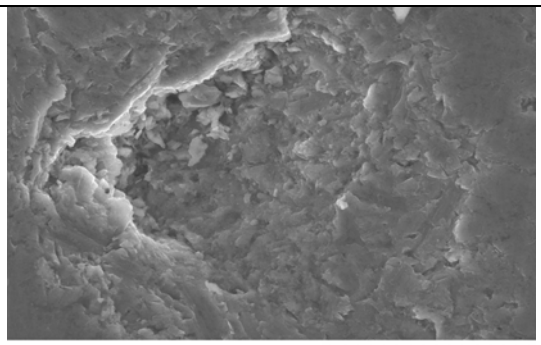

Fig.(21,a): Surface morphology for electrode II in 0.1M H_2SO_4

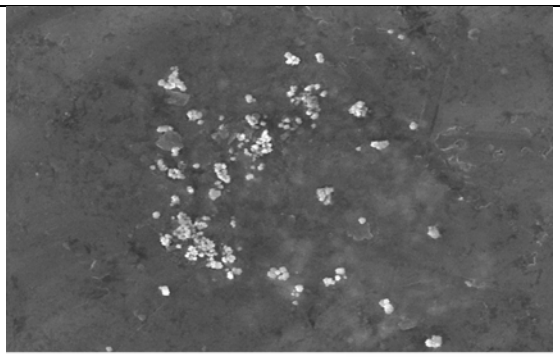

Fig.(21,b): Surface morphology for electrode II in 0.1M H_2SO_4 with addition 3% sodium dodecyl sulphate

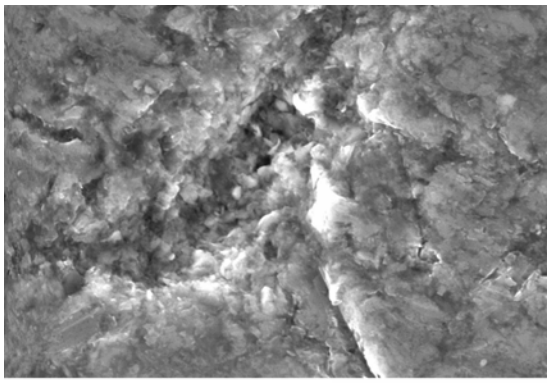

Fig.(21,c): Surface morphology for electrode II in 0.1M H_3PO_4

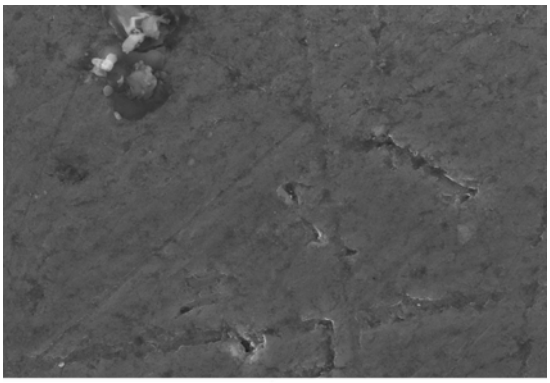

Fig.(21,d): Surface morphology for electrode II in 0.1M H_3PO_4 with addition 3% sodium dodecyl sulphate

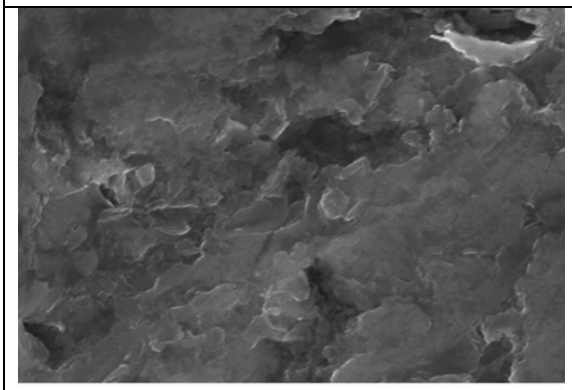

Fig.(21,e): Surface morphology for electrode II in 0.1M HNO_3

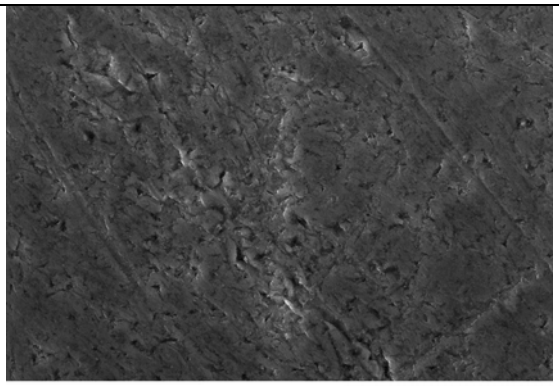

Fig.(21,f): Surface morphology for electrode II in 0.1M HNO_3 with addition 3% sodium dodecyl sulphate

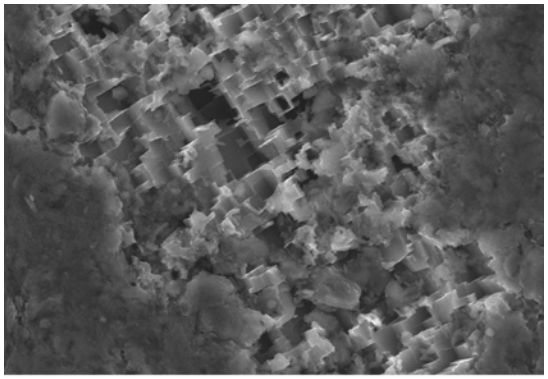

Fig.(21,g): Surface morphology for electrode II in 0.1M HCl

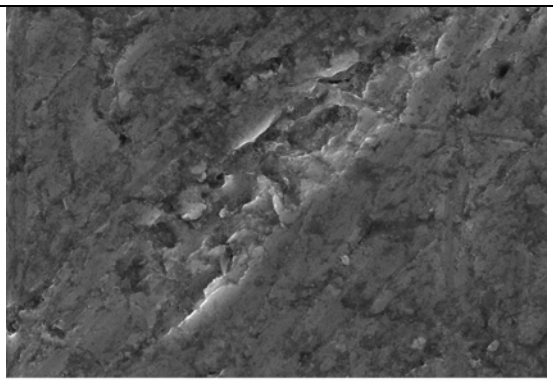

Fig.(21,h): Surface morphology for electrode II in 0.1M HCl with addition 3% sodium dodecyl sulphate

4. Conclusion:

From the mentioned results of open-circuit potential and potentiodynamic polarization measurements, it could be concluded that:

a. Open-circuit measurements showed that both immersion potential ($E_{im.}$) and steady state potential ($E_{s.s.}$) for the two electrodes depend on the nature and composition of the aluminum electrodes and electrode type I was more active than electrode type II.
b. The polarization curves have the same general features, for the two aluminum electrodes, and characterized by the appearance of active, passive and transpassive regions before oxygen evolution.
c. Electrode II becomes passive than I due to the higher Si content and formation of Al_2O_3 + SiO_2 oxide film.
d. The investigated surfactants compounds act as inhibitors for the corrosion of the two aluminum electrodes.
e. Sulfonic acid is more effective to inhibit the corrosion than sodium dodecyle sulphate.
f. Surfactant compounds adsorb on the metal surface according to Langmuir and Temkin adsorption isotherm.

References:

1. **Scaman G,M,,s, N. Birbilis and R.G. Buchheit,** Shreir's Corrosion, 3, 1974-2010 (2008).
2. **PolmearL.J.,** " Light Alloys : Metallurgy of the Light Metals" Arnold (1995).
3. **Schweitzer PA,** "Corrosion and Corrosion Protection Hand Book ", Marcel Dekker, Inc. New York and Basel, (1989).
4. **Evans U.R.,**" An Introduction to Metallic Corrosion "third Edition, Edward Arnold, London, (1981).
5. **Brasher D.M.,** Nature, London, 193, 868 (1962), "Proc, 2nd, European Symposium on Corrosion Inhibition.", Ferrara, Italy, 61 (1965).
6. **ringle J.P.S.,** Journal of Electrochemical Society , 120, p. 398 (1973).
7. **Thomas J.P., M. Fallavier, P. Spender and E. Francois,** Journal of Electrochemical Society, 127, p. 585 (1980).
8. **Khalil N. and J. S. L. Leach,** Electrochemica Acta , 31, p. 1279 (1986).
9. **Patermarakis G., P. Lenas, Ch. Karavassilis and G.Papayiannis,** Electrochemica Acta , 36, p.709 (1991).
10. **Diggle J., T. Downie and C. Goulding,** Chemical Review, 69, p. 365 (1969).
11. **Dignam M.J.,** Journal of Electrochemical Society, 112, p. 729 (1965).
12. **Evans U.R.,** " Metal Corrosion Base", translated by Zhang Keqin, Beijing, Metallurgical Industry Press, p. 396-404 (1987).
13. **Drazic D.M., S. K. Zecevic, R. T. Atanasoski and A. R. Despic,** Electrochemica Acta, 28, p.751 (1983).
14. **Sertcelik F., A. F. Cakir, M. Urgen . D. Gabe and D. Ross,** Eurocorr 97, European. Federation of Corrosion Event, 208, Trondheim, Norway, 11, p. 297-302 (1997).
15. **Critchelow G.W. and D. M. Brewis,** International Adhesion, 16(4) , P. 255 (1996).
16. **Pourbaix M.,** "Atlas of Electrochemical Equilibrium in Aqueous Solutions", 2nd ed., NACE, Housten, Texas, p.169 – 463, (1974).
17. **Nisancioglu K. and O. Lunder,** Journal of Electrochemical Society, 137 (1), 69 (1990).
18. **Parhutik V.P., IU. E. Makushok, E. Kudriavtsev, V. A. Sokol and A. N. Khodan,** Electrochemistry (Elektrokhymia), 23, p. 1538 (1987).

19. **Thomas S. and P. M. A. Sherwood,** Journal of Chemical Society Faraday Transaction, 89, p. 263 (1993).
20. **Thomas S. and P. M. A. Sherwood,** Analytical Chemistry, 64, p. 2488 (1992).
21. **Burstein G.T. and R. M. Organ,** Corrosion Science, 47, p. 2932-2955 (2005).
22. **Odynetz L.L.,** Russian Journal of Applied Chemistry, 65, p. 2417 (1992).
23. **Thompson G.E.,** Thin Solid Films, 297, p. 192 (1997).
24. **Pierre A.C. and D. R. Uhlman,** Journal of Non – Crystalline Solids, 82, p. 271(1986).
25. **Nisancioglu K. and H. Holtan,** Electrochemica Acta , 24, p. 1229 (1979).
26. **Hassel A.W. and M. M. Lohrengel,** Electrochemica Acta, 40, p. 433 (1995).
27. **Pyun S.I. , C. Lim and R. A. Oriani,** Corrosion Science , 33, p. 437(1992).
28. **Engell H.J.,** Electrochemica Acta, 22, p. 990 (1977).
29. **Song R.H., S. I. Pyun and R. A. Oriani,** Journal of Electrochemical Society, 137, p. 1703(1990).
30. **Lee S.M. and S.I. Pyun,** Journal of Applied Electrochemistry, 22, p. 151(1992).
31. **Radosevic J., M. Kliskic, P. Dabic, R. Stevenovic and A. R. Despic,** Journal of Electroanalytical Chemistry, 277, p. 105 (1990).
32. **Takahashi H., K. Kasahara, K. Fujiwara and M. Seo,** Corrosion Science, 36, p. 677 (1994).
33. **Pyun S.I. , K. H .Na, W. J. Lee and J. J. Park,** Corrosion, 56, p. 1015-1021 (2000).
34. **Branzoi V., Florentina Golgovici and Florina Branzoi,** Material Chemistry and Physics, 78, p.122-131 (2002).
35. **Nguyen T.H. and R. T. Foley,** Journal of Electrochemical Society, 126, p.1855 (1979).
36. **Moutarlier V., M.P. Gigandet, J. Pagetti and B. Normand,** Surface and Coating Technology, 161, n.2-3, p.267-274 (2002).
37. **Wood G.C. and A. J. Brock** Transaction Institute of Metal Finishing, 44, P.189 (1966).
38. **Strehblow H.H. and C.J Doherty,** Journal of Electrochemical Society, 125, p.30 (1978).
39. **Mansfeld F.,** "Corrosion Mechanism" , Marcel Dekker, New York, p.119(1987).
40. **. MaayaA.K.,** Journal of Corrosion Science and Engineering , 3, p.17 (2002).
41. **. SinghD.D.N, M. M. Singh, R. S. Chaudhary and C.V. Agarwal,** Electrochemica Acta, 26(8), p.1051-1056 (1981).
42. **FoudaA.S., A. A. Al-Sarawy, F. Sh. Ahmed and H. M. EL-Abbasy,** Corrosion Science, 51, p.485-492 (2009).
43. **Subramanyam N.S., B. S. Sheshardi and S. A. Mayanna,** Corrosion Science, 34, p. 563 (1993).
44. **Sayed Abd El-Rehim S., H. Hamdi Hassan, A. Mohammed Amin,** Materials Chemistry and Physics, 78, p.337-348 (2002).